

# Open bottom and charm production at ATLAS

*M F Watson for the ATLAS Collaboration*

*School of Physics and Astronomy, University of Birmingham, Edgbaston, Birmingham, B15 2TT, UK; supported by a Royal Society Dorothy Hodgkin Fellowship.*

## 1 Introduction

Results are presented for identified D and B mesons and b-jets, using data collected in 2010 by the ATLAS detector. The most important components of the detector for these analyses are the inner tracking detector and muon system, covering  $|\eta| < 2.5$  and  $|\eta| < 2.7$ , respectively. Events are triggered with minimum bias, muon or jet triggers, depending on the channel under consideration [1]–[6].

## 2 D meson cross-sections

Charmed hadrons are produced in the fragmentation of charm or bottom quarks, and are identified in the decay modes  $D^{*+} \rightarrow D^0 \pi_s^+ \rightarrow (K^- \pi^+) \pi_s^+$ ,  $D^+ \rightarrow K^- \pi^+ \pi^+$  and  $D_s^+ \rightarrow \phi \pi^+ \rightarrow (K^- K^+) \pi^+$ , by considering all three-track combinations with suitable kinematic cuts, e.g  $p_T$  and  $|\eta|$  of the tracks and  $D^{(*)}$  [1]. The reconstructed mass distributions are fitted to extract the number of D meson candidates, from which total cross-sections and differential cross-sections in  $p_T$  and  $|\eta|$  are extracted. The cross-sections in the kinematic range  $p_T(D^{(*)}) > 3.5$  GeV and  $|\eta(D^{(*)})| > 2.1$  are

$$\begin{aligned}\sigma^{vis}(D^{*\pm}) &= 285 \pm 16(\text{stat.})_{-27}^{+32}(\text{syst.}) \pm 31(\text{lum.}) \pm 4(\text{br.}) \mu\text{b} \\ \sigma^{vis}(D^\pm) &= 238 \pm 13(\text{stat.})_{-23}^{+35}(\text{syst.}) \pm 26(\text{lum.}) \pm 10(\text{br.}) \mu\text{b} \\ \sigma^{vis}(D_s^{*\pm}) &= 168 \pm 34(\text{stat.})_{-25}^{+27}(\text{syst.}) \pm 18(\text{lum.}) \pm 10(\text{br.}) \mu\text{b},\end{aligned}$$

where the systematic uncertainties include contributions from track reconstruction (material description), D meson selection, model dependence, signal fits, luminosity and branching ratios. Figure 1 illustrates the differential cross-sections for  $D^{*\pm}$ , in which the data are seen to lie above the NLO predictions, but within the large theoretical (scale) uncertainties.

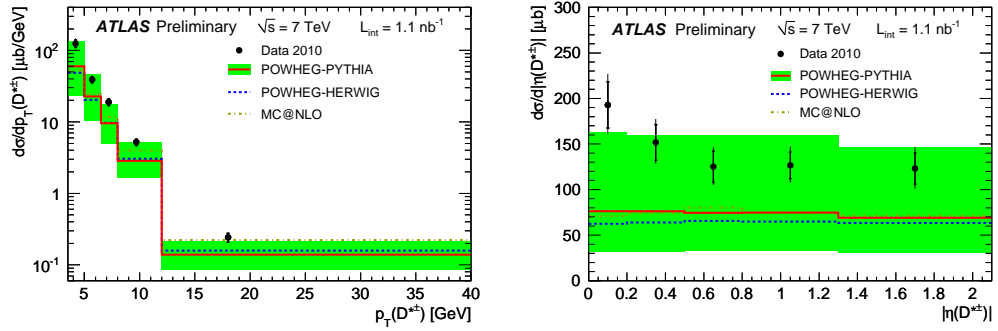


Figure 1:  $D^{*\pm}$  differential cross-sections as a function of  $p_T$  and  $|\eta|$ .

### 3 Exclusive B meson reconstruction

B mesons are reconstructed in the exclusive decay modes  $B \rightarrow J/\psi + X$ , where  $J/\psi$  decays to  $\mu^+\mu^-$  [2, 3]. Each  $J/\psi$  candidate must contain at least one “combined” muon, for which an inner detector track is matched to a track in the muon system.

In order to reconstruct the decay mode  $B^\pm \rightarrow J/\psi(\mu^+\mu^-)K^\pm$  [2], the muon tracks and an additional track are fitted to a common vertex, with a  $J/\psi$  mass constraint for the  $\mu^+\mu^-$  and the kaon mass assigned to the third track. The resulting  $m_{J/\psi K^\pm}$  mass distribution is enhanced with a transverse decay length cut and is fitted with an unbinned maximum likelihood fit (Gaussian signal and linear background) to extract the  $B^\pm$  mass and number of candidates, as seen in Figure 2. The fitted mass is consistent with expectation, and is independent of the B meson charge.

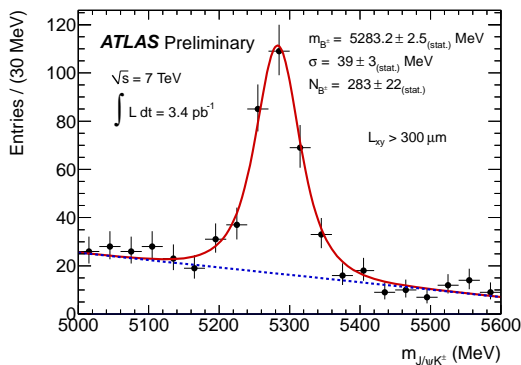


Figure 2: Mass fit for  $B^\pm \rightarrow J/\psi K^\pm$ .

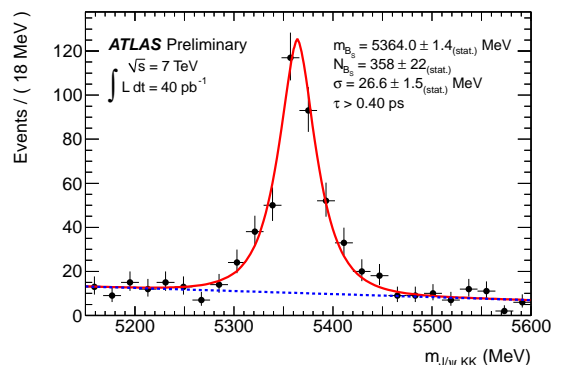


Figure 3: Mass fit for  $B_s^0 \rightarrow J/\psi \phi$ .

A similar analysis is performed for the channels  $B_d^0 \rightarrow J/\psi K^{*0}$  and  $B_s^0 \rightarrow J/\psi \phi$  [3]. Two additional tracks are combined with the  $J/\psi$  in a four-track fit, assuming the

decays  $K^{*0} \rightarrow K^+\pi^-$  or  $\phi \rightarrow K^+K^-$ . Cuts are applied to  $M(\phi)$  or  $M(K^{*0})$  and the signal is enhanced with a requirement on the decay time of the fitted secondary vertex. Figure 3 illustrates the observation of  $B_s^0 \rightarrow J/\psi\phi$  and the maximum likelihood fit to the reconstructed mass. The fitted  $B_d^0$  and  $B_s^0$  masses, both with and without decay time cuts, are consistent with expectation.

## 4 B jet cross-sections

An enriched sample of jets containing B hadrons (“b-jets”) can be obtained by requiring a displaced secondary vertex in the jet [4, 6]. Jets are reconstructed using the anti- $k_t$  algorithm with a cone size  $R = 0.4$ , then the secondary vertex (SV0) algorithm attempts to find an inclusive vertex with tracks associated to the jet, using an iterative procedure. Secondary vertices are selected with a cut on the decay length significance, relative to the primary event vertex. The b-jet fraction in a sample of tagged jets is obtained from a binned likelihood fit to the vertex mass distribution, using Monte Carlo templates. The fits are performed in bins of jet  $p_T$  and rapidity, from which the differential b-jet cross-section can be measured. Efficiency corrections are evaluated with a soft muon tagging procedure, and bin-by-bin corrections for detector effects are applied. In events containing two tagged jets, the dijet cross-section is obtained from template fits to the sum of vertex masses. The systematic uncertainties on both cross-sections are dominated by the b-jet energy scale, and the efficiency and purity of b-jet tagging.

Figure 4 illustrates the differential cross-sections and compares them to Monte Carlo predictions. PYTHIA, which includes leading order and leading logarithm terms, is found to describe the shapes but not the normalisation, while the next-to-leading order predictions of POWHEG show a steeper drop with  $p_T$  than in data. The POWHEG dijet cross-section lies above the measured values.

An alternative measurement of the b-jet cross-section uses soft muons to tag an enriched sample of b-jets [5, 6]. Muons within a cone  $\Delta R < 0.4$  from the jet axis are considered, and the distribution of muon momentum relative to the jet axis,  $p_T^{rel}$ , is fitted using templates. The b-jet fraction obtained in the fits is used to measure the differential cross-section as a function of jet  $p_T$ ; see Figure 5. This measurement of the cross-section is consistent within uncertainties with the secondary vertex measurement, and with the predictions of POWHEG.

## References

- [1] ATLAS Collaboration, ATLAS-CONF-2011-017, 12 March 2011, available at <https://twiki.cern.ch/twiki/bin/view/AtlasPublic>.

- [2] ATLAS Collaboration, ATLAS-CONF-2010-098, 16 November 2010.
- [3] ATLAS Collaboration, ATLAS-CONF-2011-050, 1 April 2011.
- [4] ATLAS Collaboration, ATLAS-CONF-2011-056, 4 April 2011.
- [5] ATLAS Collaboration, ATLAS-CONF-2011-057, 11 April 2011.
- [6] References [4] and [5] have been updated and combined in “Measurement of the inclusive and dijet cross-sections of b-jets in pp collisions at  $\sqrt{s} = 7$  TeV with the ATLAS detector”, arXiv:1109.6833 [hep-ex], submitted to EPJC (Sept. 2011).

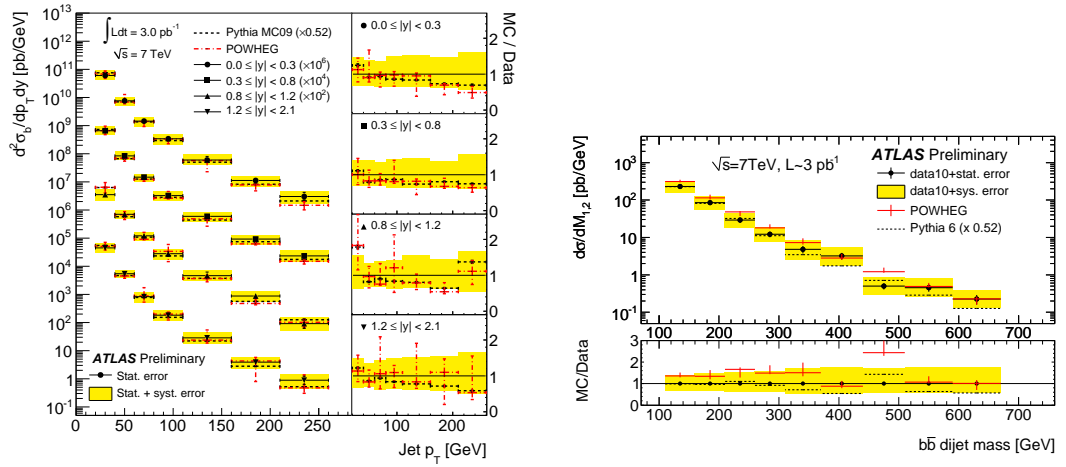


Figure 4: b-jet cross-section (left) and  $b\bar{b}$ -dijet cross-section (right). The PYTHIA predictions are scaled by 0.52.

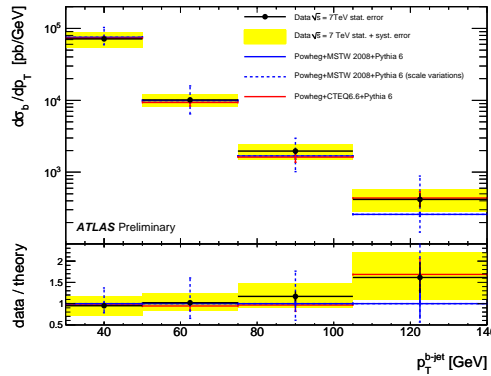


Figure 5: b-jet cross-section using the  $p_T^{rel}$  method.